# RECURSIVE MULTI-OBJECTIVE OPTIMIZATION OF MARS-EARTH-VENUS TRAJECTORIES

**Kirk S. S. Barrow**[1] *, **Marcus J. Holzinger**[1]†

[1] ***Georgia Institute of Technology, Atlanta, Georgia, 30332, United States***

The NASA exploration roadmap envisions a sustainable human presence beyond Earth orbit with an emphasis on Mars habitation. Establishing an interplanetary transportation system in orbits that periodically intersect Earth and Mars have been under study since 1969 to meet this end, but solutions generally suffer from high $\Delta v$ requirements, high approach velocities, and unfeasibly long transit times or impractical simplifying assumptions like co-planar, circular orbits. This work seeks to expand investigations to connective low-thrust, low-$\Delta v$ trajectories that also take advantage of Venusian gravity assists when available to further optimize cyclic systems. By leveraging supercomputing resources, this work also seeks to diverge from studies using cycler templates and explore a larger parameter space for potential solutions that take advantage of realistic planetary ephemeris like plane change maneuvers. To optimize the process, a piecewise multi-objective Newton's method optimization is applied to combinations of planets resulting in several tours per year with less than 7 km/s $\Delta v$ including Earth departure $v_\infty$. This method is demonstrably better than an even sampling of launch and encounter dates for investigations with limited computational resources. The inclusion of Venus allows the algorithm to take advantage of fortuitous alignments of Venus for plane change maneuvers, reducing the overall cost. Venusian-inclusive tours also provides launch opportunities outside the usual Earth-Mars launch windows.

## INTRODUCTION AND BACKGROUND

The logical predecessors to n-body connective trajectory analysis for low $\Delta v$ continuous spacecraft transportation between Earth and Mars are cycler trajectories. These trajectories are a class of orbits connecting Mars and Earth in a regularly repeating pattern and have been under study since at least 1969 with the work of Rall.[1,2] The use and study of these trajectories was later popularized by former astronaut Buzz Aldrin[3] who suggested that a solution connecting Earth and Mars existed that repeated every synodic period in 1985. The one synodic period Earth-Mars cycler, nicknamed the "Aldrin cycler," was confirmed by Byrnes et. al.[4] in 1993 along with several investigations into other orbits by Friedlander et. al.[5] and Brynes et al.[6]

Using a series of simplifying assumptions including circular, in-plane orbits for both Earth and Mars, McConaghy and Longuski[7] generate an exhaustive list of connective orbits of up to four synodic periods and seven revolutions by using gravity assists at Earth encounters and patching together trajectories. Using the GALLOP tool,[8,9,10,11] McConaghy et. al.[12] extended the study to realistic planetary ephemeris for two-synodic period cyclers. Their work was subsequently extended to three-synodic period cyclers by Chen.[13] Both solutions use the possibility of intermediate impulse maneuvers to rectify the co-planar cycler templates with the realistic planetary ephemeris. Using a similar template strategy, Russell and Ocampo[14] investigate using analytically calculated partial derivatives with SNOPT[15] to generate promising near-ballistic trajectories with low arrival velocities at both bodies from template cyclers. They produce a comprehensive list of cyclers with well minimized $\Delta v$ costs for a range of launch years and cycler classes. While these results provide an extensive overview of repeating connective trajectories between Earth and Mars, they do not nec-

*Graduate Student, School of Physics, kssbarrow@gatech.edu

†Assistant Professor, School of Aerospace Engineering, holzinger@gatech.edu

essarily explore the full parameter space of promising trajectories between the two planets nor is their method extensible to the inclusion of more planets in a Solar System tour.

This work proposes to explore classes of trajectories that take advantage of gravity assists from Earth, Mars, and Venus to explore optimization of the required $\Delta v$, hyperbolic excess velocities on encounters with Earth and Mars, and Earth-Mars transit times with respect to the ephemeris-based gravity assisted Mars-Earth Aldrin cycles described by both Russell and Chen. The contradictory requirement for low times of flight, low arrival velocities, and low spacecraft $\Delta v$ for most robotic and human spaceflight applications requires a substantial optimization effort of trajectories and a flexible parameter space. Therefore, the use of a template cycler is abandoned in favor of an open-ended simultaneous optimization of gravity-assisted trajectories and transit times over a large number of launch dates. This approach is inherently computationally expensive so an algorithm that recursively minimizes the cost of a tour of planets incrementally is developed. To help expand the solution space, a flexible solution-finding approach that allows the transition between cyclers and seizes fortuitous alignments to make or avoid a plane changes is applied.

This work contributes a) a novel optimization approach for many-planet gravity assist trajectories, b) new classes of solutions for Mars-Earth transportation, and c) a multi-objective optimization of time of flight, hyperbolic excess velocity, and $\Delta v$ for hundreds of potentially feasible tours.

## APPROACH

Due to the introduction of Venus into the analysis, an exhaustive analysis of possible connective trajectories that include repeated encounters between Earth and Mars requires the investigation of several branching solutions which must be independently optimized against a cost function. The total $\Delta v$ of an individual tour, which is calculated as the required thrusted change in velocity of the spacecraft including the hyperbolic excess velocity needed to initially depart Earth, and the time-of-flight are minimized by numerically-determined second order partial derivatives of cost with respect to encounter times. Each planetary body is assumed to contribute the possibility of a ballistic or powered gravity assist. Additionally, a low thrust trajectory that results in the same encounter dates at each planetary body is calculated using iterative local linearization by method of a state transition matrix for use in relevant applications.

### Optimization Hierarchy

*Cost Function* The cost of the three-planet optimization of a multi-planetary tour is calculated to account for the total trip $\Delta v$, the time of flight, and the hyperbolic excess velocity. The time of flight cost is taken to be the mean of the average time since the last Earth encounter to the next Mars encounter and the average time since the last Mars encounter to the next Earth encounter. The hyperbolic excess velocity cost is taken to be the mean of the average Earth departure and Mars arrival $v_\infty$. These three factors are reasoned to be the most pertinent in an interplanetary human transportation system and the cost of a trajectory is therefore calculated using the multi-objective cost function of the form

$$J = w_0 \left( \frac{1}{n} \sum_{i=1}^{n} \Delta v_i \right) + w_1 \left( \frac{1}{m} \sum_{i=1}^{m} \mathrm{TOF}_{\mathrm{M-E,i}} + \frac{1}{\mathrm{p}} \sum_{\mathrm{i=1}}^{\mathrm{p}} \mathrm{TOF}_{\mathrm{E-M,i}} \right) + w_2 \left( \frac{1}{q} \sum_{i=1}^{q} \Delta v_{\mathrm{E+,i}} + \frac{1}{r} \sum_{i=1}^{r} \Delta v_{\mathrm{M-,i}} \right) \tag{1}$$

where $w_0$, $w_1$, and $w_2$ are the weights for calculation of $\Delta v$, time of flight, and hyperbolic excess velocity respectively. Weights are changed as required to explore the entire solution space. The cost is constructed to be an implicit function of a column matrix of encounter times at each planet in J2000 time units.

*Selection of Planets* Useful combinations of planets are calculated using a Cartesian product of the planets Earth, Mars and Venus allowing $n - 2$ repetitions where $n$ is the number of planets. These combinations are then culled to planet lists that offer a predetermined number of Earth-Mars and Mars-Earth encounters after appending Earth to beginning and end of each combination. To explore possible launch and subsequent encounter dates, an even sampling of Earth departure dates is assigned to each processor for each combination

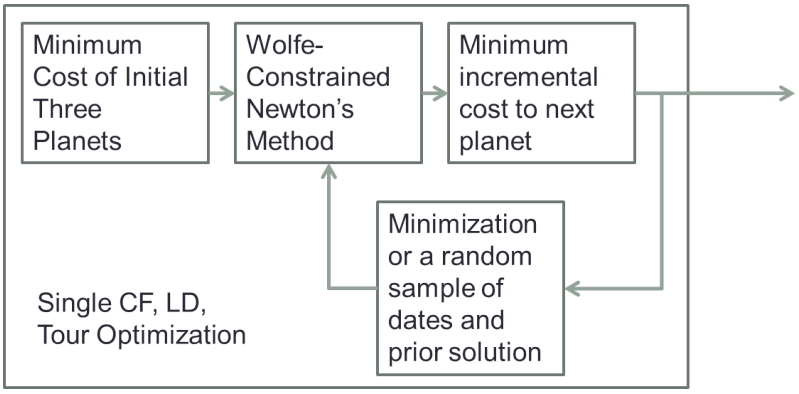


**Figure 1. Flow chart of optimization loop for a single combination of planets and for a single launch date and a single combination of cost function weights.**

of planets. Then, an even sampling of transit times between one fifth of a year and two and a half years are conducted to search for a minimum cost to the next two planets using a gravity assist maneuver at the second planet. Minima for each launch date and the first three planets in each combination are stored and used as initial guesses in the optimization process.

*Optimization Loop* From the initial guess for the encounter times of the initial three planets, another minimum for an incremental fourth planet is again calculated using an even sampling of transit times. Due to the piecewise nature of this search and the propensity of any minima to be local in nature, a random sampling of encounter times with a flat distribution about the initial guess is explored to provide flexibility between adjacent concave regions of the cost. The best cost between the even sampling and random sample is selected to begin a second order quadratic optimization using the first and second partial derivatives of the cost with respect to a column matrix of the encounter times.

The optimization root-finding equation is given as

$$\mathbf{t}_{i+1} = \mathbf{t}_i - \gamma[\mathbf{H}f(\mathbf{t}_i)]^{-1}\nabla(\mathbf{t}_i) \tag{2}$$

where $\mathbf{t}$ is the list of encounter dates, $\mathbf{H}$ is the Hessian of partial derivatives, and $\gamma$ is a scaling parameter which is limited iteratively during descent to satisfy the Wolfe conditions.[17] These are given as

$$\mathbf{p}_i = \gamma[\mathbf{H}f(\mathbf{t}_i)]^{-1}\nabla(\mathbf{t}_i) \tag{3}$$

$$f(\mathbf{t}_i + \alpha_i\mathbf{p}_i) \leq c_1\alpha_i\mathbf{p}_i^T\nabla f(\mathbf{t}_i) \tag{4}$$

$$|\mathbf{p}_i\nabla f(\mathbf{t}_i + \alpha_k\mathbf{p}_i)| \leq c_2|\mathbf{p}_i^T\nabla f(\mathbf{t}_i)| \tag{5}$$

where $c_1$ and $c_2$ are weights set to $1\times10^{-6}$ and 0.9 respectively to encourage convergence and $\alpha$ is the step length. If the conditions cannot be applied, the initial guess is taken to be the minimum. Else, the optimization terminates after twenty successful descents or when each step reduces the cost by less than $1 \times 10^{-6}$.

This result serves as the initial guess for the addition of the next planet which undergoes the same process including the minimization against random encounter times and the full optimization iteration. This is shown in Figure 1 and later demonstrated in more detail.

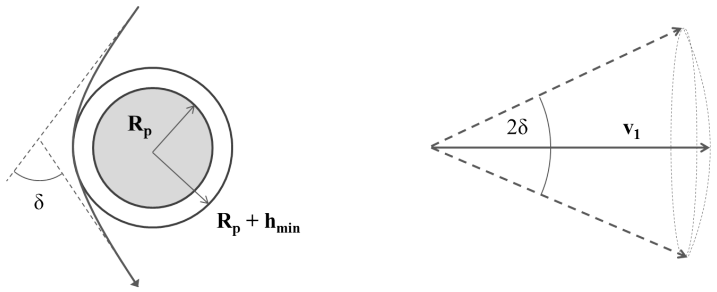


**Figure 2. Inner radius of impact parameters about a planet (left) and possible turn angles for an arrival $\vec{v_1}$ (right) given possible impact parameters outside of $R_{\mathrm{p}} + h_{\mathrm{min}}$.**

**Gravity Assist Optimization**

Assuming the availability of a gravity assist, a broad range of possible velocity states are available after each planetary encounter. These available states are dependent on the position and velocity of the planet in its orbit so fundamentally, optimizing trajectories that use gravity assist require the optimization of both the targeted time of encounter and the maneuver itself. While solutions that exactly connect planets ballistically may be preferred, they cannot be assumed to be available and thus accounting for the possibility of either a position error or velocity error is explored.

*Optimizing with Respect To Velocity Error* Gravity assist maneuvers take advantage of the gravity of a body to rotate the arrival $v_\infty$ by some angle determined by the mass of the body and the impact parameter. By enforcing a final position state for the spacecraft, gravity assist maneuvers can be optimized to minimize the required change in velocity needed to accomplish both the rotation and change in magnitude that results in a Keplarian trajectory towards an encounter with the next planet at a given time. Since gravity assist-maneuvers are an extension of a hyperbolic two-body orbit and cannot change the magnitude of a hyperbolic excess velocity, a $\Delta v$-minimized maneuver can only change the magnitude of the sun-centered velocity by method or rotation of the excess velocity vector. The possible rotation angle, $\delta$, is given by

$$sin\left(\frac{\delta}{2}\right) = \frac{1}{1 + r_p v_\infty^2/\mu_{planet}} \tag{6}$$

The minimum distance to the planet $r_p$ used in this analysis is the sum of the mean equatorial radius and a standoff distance of 500, 300, and 150 km for Venus, Earth, and Mars respectively. It is assumed that an approaching spacecraft can easily adjust the encounter trajectory so that the gravity assist maneuver turns the arrival $\vec{v_\infty}$, $\vec{v_1}$, in any direction within a cone of possible final $\vec{v_\infty}$, $\vec{v_2}$, directions that subtends an angle of $2\delta$. The algorithm enforces that the final velocity magnitude after the maneuver must match the required free-fall velocity to reach the target body and any changes in magnitude must occur before reaching the sphere of influence of the encounter body. Using the final magnitude as the radius of a spherical sector centered on the final velocity direction with subtending $2\delta$, the minimum change in velocity required of the spacecraft is the minimum difference between $\vec{v_2}$ and the outer surface of the sector as demonstrated below. For reference, the $l^2$-norm of a vector is hereafter abbreviated as $||\vec{x}|| = x$ for any vector $\vec{x}$.

Figure 3 (bottom right) shows a two dimensional cross section of a rotated spherical coordinate system centered at the vertex of the vectors with the positive z-axis along the direction of $\vec{v_2}$ and the positive x-axis upward in the plane of the diagram. To minimize $\Delta v_e$, an objective function $f(\vec{x})$ is minimized with equality and inequality constraints using a Lagrange multiplier.

$$\vec{v_1} = \vec{v_1}(v_1, \theta_1, \phi_1), \vec{v} = \vec{v}(v, \theta, \phi_1) \tag{7}$$

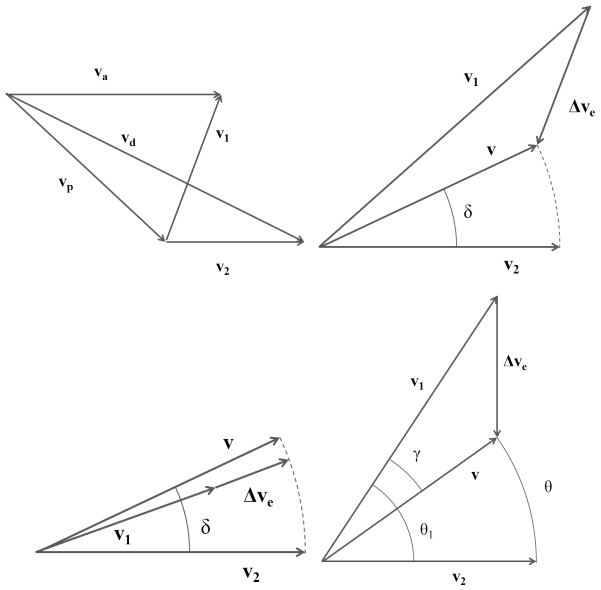


**Figure 3. Gravity assist geometry diagrams showing the calculation of $\Delta\vec{v_e}$ from arrival and departure velocities $\vec{v_a}$ and $\vec{v_d}$ where $\vec{v_p}$ is the orbital velocity of the planet. Also shown is a reference figure with variable names for the proof (bottom right).**

$$g(\vec{x}) = v - v_2 = 0 \tag{8}$$

$$h(\vec{x}) = \theta \leq \delta \tag{9}$$

$$f(\vec{x}) = ||\vec{v}_1 - \vec{v}||^2 = v_1^2 + v^2 - 2v_1 v cos(\gamma) = v_1^2 + v^2 - 2v_1 v cos(\theta_1 - \theta) \tag{10}$$

By the Karush-Kuhn-Tucker conditions, the following equations and inequality are satisfied for the extrema of $f(\vec{x})$.

$$\nabla f(\vec{x}) - \lambda \nabla g(\vec{x}) - \mu \nabla h(\vec{x}) = 0 \tag{11}$$

$$\mu(\theta - \delta) = 0, \mu \geq 0 \tag{12}$$

These conditions and constraints are sufficient to find unique classes of general solutions that minimize $v_e$. Equation 11 provides the following system of equations after taking the gradient.

$$2v_2 - 2v_1 cos(\theta_1 - \theta) - \lambda = 0 \tag{13}$$

$$2v_1 sin(\theta_1 - \theta) - \mu / v_2 = 0 \tag{14}$$

From Equation 12 either $\mu = 0$ or $\theta = \delta$. When $\mu = 0$, Equation 14 reduces to

$$sin(\theta_1 - \theta) = 0 \tag{15}$$

$$\theta = \theta_1 + n\pi, n \in \mathbb{Z} \tag{16}$$

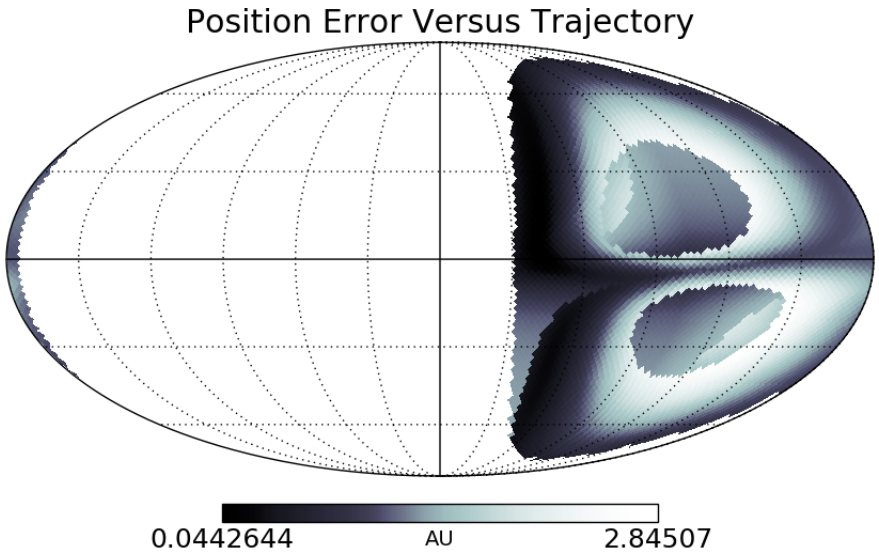


**Figure 4. Position error for an example arrival velocity vector showing the possible departure vectors and errors for an unthrusted gravity assist maneuver.**

All values of $n$ except 0 are rejected by reasoning that odd values of $n$ correspond to maxima and even values of n are coincident with the solution where $n = 0$. Thus the solution $\theta_1 = \theta \leq \delta$ is obtained when combined with Equation 9 to accommodate the range of possible gravity assist maneuvers. This implies that if the initial angle between $\vec{v_1}$ and $\vec{v_2}$ is less than $\delta$, only the length of the vector changes from $v_1$ to $v_2$ with no change in the polar angle.

When $\theta = \delta$, Equation 14 reduces to

$$2v_1v_2sin(\theta_1 - \delta) = \mu \tag{17}$$

Since $\mu \geq 0$ and solutions in quadrant III and IV are again eliminated when seeking a minimum, the condition $\theta_1 \geq \delta$ must correspond to the solution $\theta = \delta$. This implies that if $\theta_1$ is greater than the maximum gravity assist turn angle $\delta$, $\Delta\vec{v_e}$ is both a change in magnitude from $v_1$ to $v_2$ and change in polar angle of exactly $\theta_1 - \delta$ towards the positive z-axis. The resulting $\Delta\vec{v_e}$ orientations are shown in Figure 3.

Thus the required thrusted encounter velocity change, $\Delta\vec{v_e}$, is either a maneuver to change the velocity magnitude or the difference between $v_{\infty,a}$ and the edge of the sector displaced a full $\delta$ from $v_{\infty,d}$, depending on whether the angle between the two $v_\infty$ vectors is less than or greater than $\delta$ respectively.

*Optimizing with Respect to Position Error* By assuming $\Delta\vec{v_e}$ and constraining the departure to unassisted gravity turns and allowing the encounter time to vary, it is possible to optimize with respect to a minimized miss distance at the third planet. Figure 4 shows an ecliptic histogram of the position error given the allowable zero-thrust departure angles from a planet in a sample scenario. Miss distances of zero are preferable and it is assumed that the lowest miss distance also corresponds to the most desirable trajectory and corresponding set of encounter dates.

**Universal Time of Flight and Gauss's Problem**

To simulate connective trajectories between planetary bodies, a patched conic method is employed assuming two-body dynamics throughout the flight of a spacecraft including during encounters with planetary bodies. This simplifying assumption allows the use of well-established time-dependent iteration algorithms for the location of an object traveling along a gravitationally-induced conic section. Specifically, solutions

to the Gauss Problem and the Lambert Problem and are used extensively in this work and are thus briefly described along with the particulars of their implementation.

*Gauss's Solution to Lambert's Problem (p-iteration)* The determination of an orbit from two specified position vectors and a fixed time-of-flight is called Lambert's problem. In contrast to Lambert's own solution which is computationally sensitive to small transfer angles between the initial position vectors, Guass's solution requires no careful treatment of special cases and is therefore used in this study. Guass' solution takes advantage of the direct monotonic relationship between the semi latus rectum and the orbital time of flight of an object in two-body motion when one body is sufficiently large to allow the mass of the larger object to approximately act as a non-accelerating inertial reference frame. Given two position vectors and a time of flight, one may therefore iterate estimates of the semi-major axis and the semi latus rectum until achieving convergence with the desired time-of-flight. Due to the ambiguity of the short or long flight path between the given position vectors, each set of initial conditions yields as many as two unique solutions or as few as none in special cases.

In practice, convergence to a relative error of $1 \times 10^{-9}$ is achieved in as little as 6 iterations and thousands of such calculations can be completed within a few seconds on a single processor. There are two singularities in the relationship between the semi latus rectum and the semi-major axis which can cause difficulty with an improperly chosen initial guess. When the code fails to converge, an initial semi latus rectum guess closer to the singularity usually decreases the step-size and allows for convergence. Code for this study attempts this four times before assuming that no useful solution exists. Once the orbit has been determined, the initial and final velocity vectors can be calculated using functions of the orbital elements. The utility of this approach for this project is an ability to determine trajectories between bodies with known positions such as planets since the mass of the sun roughly satisfies the two body inertial frame requirement.

*Universal Variable Formulation For Time of Flight* The universal variable formulation of Kepler's time-of-flight (UTOF) solution is so named due to its use of a single variable for hyperbolic, parabolic, and elliptic orbits and was first derived by Bate.[17] Given an initial position and velocity vector and a given time of flight, the mean motion and the universal variable are iterated until convergence. If successful, the final position and velocity state of the body can again be determined with the known orbital parameters, using functions of the orbital parameters and their derivatives.

While UTOF is powerful tool for determining the location of celestial bodies and spacecraft as a function of time, it suffers from numerical precision and convergence errors for longer times of flight. As with the p-iteration algorithm, convergence is sensitive to the initial guess for the universal variable and four attempts are made before the possibility of a useful solution is ruled out. For longer times of flight, the trajectory is segregated into two or more parts as needed. Because the p-iteration and UTOF techniques both have the final velocity as an output, they may be used in conjunction as an error checking tool.

The theoretical framework for the UTOF and p-iteration codes are constructed in agreement with a Bate, Mueller, and White text.[18] Python and numpy (which handles arrays using an efficient underlying C algorithms) are chosen as the scripting languages for all simulations. Each section of code is segregated into helper functions and wrapper functions at logical breaking points to allow recursion and to aid multi-threading.

*Planetary Positions* Princeton University[19] provides a list of orbital elements for the major bodies in the solar system and their time of periapsis near Jan 2006. Assuming that the orbits of the planets repeat exactly every orbital period, the position of the planets are propagated forward from their most recent periapsis using the UTOF algorithms to determine their position at an arbitrary point in time.

Since both the p-iteration and UTOF codes depend on factors of the square root of $\mu = GM$, computational time and numerical error is reduced by introducing a canonical coordinate system where $\mu_\odot = 1\ \mathrm{DU}^3/\mathrm{TU}^2$. The distance unit (DU) is taken to be 1 AU and thus assuming two-body Keplarian motion with an inertial reference frame fixed to the center of the sun, the time unit must be 1 year/$2\pi$ and the velocity unit is 1 DU/TU $\approx 29.79 km/s$. The code internally converts between time units, seconds, and dates as needed. These orbits are found to be consistent with the orbital period times provided by Princeton.

Therefore the optimization algorithm can be summarized with the pseudocode given in Algorithm 1 with

| Orbital Element | Venus | Earth | Mars |
|---|---|---|---|
| a (AU) | 0.723336 | 1.000003 | 1.52371 |
| e | 0.00678 | 0.001671 | 0.09339 |
| $\Omega$ (deg) | 76.7 | N/A | 49.6 |
| i (deg) | 3.3947 | 0.0 | 1.850 |
| $\omega$ (deg) | 54.9 | 102.9 | 286.5 |
| $t_p$ | 2006 Oct 06, 05:19 UTC | 2007 Jan 15, 00:30 UTC | 2007 Jun 01, 07:20 UTC |

logical commands capitalized for clarity.

**Algorithm 1** Recursive Opitmization of Tour Cost

```
for w0,w1,w2 in [0,0.1,...,0.9,1] do
    for all planetary combinations (1, 12, and 86 for 7, 8, and 9 planet tours respectively) do
        for 60 launch dates per year do
            for an even sample of encounter dates to the second planet do
                if NOT taking a derivative AND finding an initial cost before descent then
                    for a large even sample of gravity turn angles at the second planet do
                        Use UTOF and p-iteration to find the miss distance for each turn angle
                        Determine the corresponding encounter time to the third planet
                    Add the encounter time corresponding to the minimum miss distance to the sample
                    Add an even sample of encounter dates at the third planet
                Use UTOF and p-iteration to find the cost of each set of encounter times
                # The interior of the loop above is hereafter used to determine cost.
            Randomly sample encounter times for a lower cost
            Use the best-cost encounter time sequence for the following descent loop
            while NOT converged AND descents ≤ 20 do
                Find the first and second derivatives of cost with respect to encounter times
                Calculate the descent direction
                Vary the step size up to 40 times to satisfy the Wolfe conditions
                Descend
                # The loop above is hereafter used to descend to a minimum cost.
            while number of planets ≤ length of tour do
                Add an even sample of encounter times to the next planet
                Determine cost by chaining cost calculations for multiple gravity assists
                Randomly sample encounter times for a lower cost
                Descend to a cost minimum
```

### Low Thrust Optimization

Each planetary tour collected in the main algorithm corresponds to an idealized impulse solution assuming powerful rockets are available to impart a significant change in velocity at the point of encounter. Reasoning that the optimized impulse solution corresponds roughly with the tour and launch date of the best low thrust trajectory solution, useful tours are studied to determine low thrust alternatives.

Low thrust trajectories are built under the assumption that their goal is to achieve $\Delta\vec{v_e}$ with a minimized continuous thrust solution. These solutions are constructed to achieve the required change in velocity before the planetary encounter such that the spacecraft is on a free-fall trajectory to the next encounter after the gravity assist. Therefore no thrust is used on the final leg of a tour. The encounter time at all planets is held constant with respect to the solution generated in the planetary tour algorithm.

To calculate low thrust trajectories, a linearization and discretization of the trajectory is performed starting from the Cartesian equations of motion (Equation 18) where the origin is taken to be the position of the sun.

$$\dot{\vec{x}} = \frac{-1}{x^3}\vec{x} + \mathbf{B}\vec{u} \tag{18}$$

Thus the time derivative of the state vector $\dot{\vec{x}}$ is the sum of $\mu$-normalized function of the state and time $f(t, \vec{x})$ and the constant control matrix $\mathbf{B}$ acting on the thrust vector $\vec{u}$. Treating $\Delta\vec{v_e}$ as a small variation in the final state allows a first order approximation of the relationship between the initial variation in state to the final variation in state. This is taken with respect to the free-fall trajectory under gravitation attraction.

$$\delta\vec{x_f} \approx \Phi(t_f, t_i)\delta\vec{x_i} \tag{19}$$

$$\Phi(t_f, t_i) = e^{\int_{t_i}^{t_f} \frac{\partial f}{\partial \vec{x}} d\tau} \tag{20}$$

Under thrust, Equation 19 expands to Equation 21 where $\delta\vec{u}$ is the variation in thrust from the ballistic solution.

$$\delta\vec{x_f} \approx \Phi(t_f, t_i)\delta\vec{x_i} + \Gamma(t_f, t_i)\delta\vec{u_i} \tag{21}$$

$$\Gamma(t_f, t_i) = \int_{t_i}^{t_f} \Phi(t_f, \tau)\mathbf{B}d\tau \tag{22}$$

$$\delta\vec{x_f} = \Phi(t_{\mathrm{N}}, t_0)\delta\vec{x_0} + [\Phi(t_{\mathrm{N}}, t_1)\Gamma_1, \cdots, \Gamma_{\mathrm{N}} \cdots \Gamma_1\delta\vec{u_{\mathrm{N}}}] \begin{bmatrix} \delta\vec{u_1} \\ \vdots \\ \delta\vec{u_{\mathrm{N}}} \end{bmatrix} \tag{23}$$

$$[\Phi(t_{\mathrm{N}}, t_1)\Gamma_1, \cdots, \Gamma_{\mathrm{N}} \cdots \Gamma_1\delta\vec{u_{\mathrm{N}}}]^{-1}[\delta\vec{x_f} - \Phi(t_{\mathrm{N}}, t_0)\delta\vec{x_0}] = \begin{bmatrix} \delta\vec{u_1} \\ \vdots \\ \delta\vec{u_{\mathrm{N}}} \end{bmatrix} \tag{24}$$

$$\delta\vec{x_0} = \vec{0}, \delta\vec{x_f} = \begin{bmatrix} \vec{0} \\ \Delta\vec{v_e} \end{bmatrix} \tag{25}$$

$$\vec{x}_{\mathrm{low-thrust,k}}|_{t_i} = \vec{x}_k|_{t_i} + \delta\vec{x}_{ik}|_{t_i} \tag{26}$$

The variation in state is calculated incrementally to allow for a time varying solution for $\vec{u}$ where each initial state in each increment is the final state of the previous increment and thrust is constant between. Thus by using $\Delta\vec{v_e}$ as the total change in the velocity state and enforcing no change in the position state, the locally linearized solution to the required thrust can be solved directly and iterated to convergence. This solution is taken as an approximation of the required trajectory and the total $\Delta v$ required for a tour and used only for comparisons with other tours.

### Even Sampling Base Case

The method of piecewise optimization of trajectories is the result of a trade-off between the complete sampling of the solution space of encounter times and the need for restraint in the use of computational time. Using approximately the same computational time, an alternate method of even sampling is applied for comparison.

After launching from Earth, 200 transit times from 0.2 to 2 years (3.28 days/increment) after the launch date at Mars and Venus are explored using the p-iteration algorithm. Subsequently another 200 arrival dates that connect the trajectory to the third planet, which may be either Earth, Mars, or Venus, 0.2 to 2 years after arrival to the second planet are explored. With a three-planet trajectory established, the spacecraft $\Delta\vec{v_e}$ is calculated and stored along with the state at the final planet. At this point the minimum solution for the sum of launch $v_\infty$ and $\Delta\vec{v_e}$ for each three-planet tour is selected to explore branching solutions for subsequent legs. Ideally, minimization is held until the end of the tour, but available computing resources and the limited scalability requires consolidation of the solution space to one solution for each of the 100 initial launch dates and combination of planets after every three encounters.

For the next leg of the tour, $\Delta\vec{v_e}$ are calculated for the third and fourth planets and optimized at the arrival at the fifth and so on with optimizations every three planets. Since each encounter increases the number of branches, minimized solutions with high velocity requirements and a small number of legs connecting Earth and Mars are culled to allow computation of up to nine planetary encounters. Finally, the cheapest tour for each planet combination of the 100 initial launch dates is stored for study.

### Approach Comparisons

*Chen et al. (2005)* In a search for three-synodic period Earth-Mars cyclers, Chen et al.[13] apply a method to stitching together semi-cyclers to generate longer tours. By using the GALLOP algorithm which is driven by the Sparse Nonlinear Optimizer (SNOPT) package,[15] five-planet cyclers calculated from co-player circular orbits and are optimized using realistic planetary ephemeris. The method of piecewise optimization of five planets is conceptually similar to the base case explored in this work and results in $\Delta v > 12$ km/s for eight Earth-Mars legs without including Earth departure hyperbolic excess velocity. By discretizing trajectories into locally-linearized segments to create a low thrust solution, five-planet segments are directly optimized for low thrust solutions where this work uses low thrust solutions as a post-processing treatment of an optimized impulse trajectory. Chen et. al note that optimizing a low thrust solution for the entire tour is computationally infeasible, requiring thousands of optimization variables for even a course discretization.

*Russell and Ocampo (2006)* Russell and Ocamapo[14] use a gradient descent method to optimize the $\Delta v$ of template cyclers using SNOPT. Like this work, they calculate the required $\Delta v$ by taking advantage of gravity assists at Earth and Mars. Analytic gradients are calculated for the position and time constraints with respect to the unknown time, hyperbolic excess velocities, and final positions, and are minimized until convergence. A cost function that adds the trip $\Delta v$ and miss distances is employed if the constraints cannot be satisfied. Several ballistic or low cost tours are calculated, but the solution set is restricted to a predetermined set of Earth-Mars cyclers of various synodic periods.

Russell and Ocampo's approach differs from this work in that instead of analytically determining partial derivatives of the unknowns with respect to physical constraints, numerical partial derivatives of the cost with respect to encounter time are calculated directly. Furthermore, the addition of randomization leverages more of the benefits of a genetic algorithm, allowing solutions to migrate between minima when ballistic trajectories cannot be found. Furthermore, since no cycler templates are used in this work, several previously unexplored solutions sets are discovered. A disadvantage of this approach with respect to those of Russell and Ocampo is difficulty optimizing specific trajectories and reproduction due to randomization.

*McConaghy (2006)* McConaghy[12] uses SNOPT to optimize two-synodic period cycler trajectories. Using template cyclers calculated from co-planar circular orbits, orbital elements are varied until they serve as appropriate initial guesses for an ephemeris model. Because there are two more unknowns than the number of constraint equations, the solutions are not unique and generate a two dimensional space of feasible initial

| Encounter | Planet | Encounter Date | $\Delta v_{\mathrm{req,impulse}}$ | $\Delta v_{\mathrm{req,low-thrust}}$ |
|---|---|---|---|---|
| 1 | Earth | June 20, 2018 | 5.38 km/s | 5.38 km/s |
| 2 | Mars | September 23, 2018 | 0.06 km/s | 0.09 km/s |
| 3 | Earth | July 3, 2020 | 0.04 km/s | 0.06 km/s |
| 4 | Mars | March 19, 2021 | 3.62 km/s | 4.59 km/s |
| 5 | Earth | September 30, 2022 | 0.12 km/s | 0 .15 km/s |
| 6 | Mars | March 3, 2023 | 0.00 km/s | 0.00 km/s |
| 7 | Earth | October 13, 2024 | N/A | N/A |
| Total | | | 9.23 km/s | 10.26 km/s |

**Table 1. Seven planet Earth-Mars cycler used as a basis for comparison with the expanded parameter space. The initial Earth departure $\Delta v$ is the required velocity in excess of the orbital velocity of the Earth about the sun to attain the optimized trajectory to the next planet. Each subsequent $\Delta v$ are maneuvers performed during encounters to remain on the cycler.**

launch and final arrival dates. However the encounter dates for bodies in the middle of the tour are found to vary little in the sample and it is reasoned that these dates represent the encounter times that would be consistent with an "ideal" cycler. Thus the arrival and launch dates can be varied to minimize other parameters such as launch hyperbolic excess velocity. Arrival and departure hyperbolic excess velocities constrained to be equivalent and any required $\Delta v$ comes from an impulse maneuvers between planets.

Trip $\Delta v$ for the first nine planets are comparable to this work, but generally exhibit longer times of flight. To minimize times of flight McConaghy applies their approach to initial guess with ten-day increments of time of flight to search for low $\Delta v$ solutions. This work optimizes time of flight in the cost function and offers a more extensive and flexible solutions space while McCanghy offers solutions that can be optimized for planet-to-cycler rendezvous $\Delta v$ independently.

## RESULTS

Since 2018 is a Mars-Earth Hohmann Transfer launch window year and examples of cycler trajectories with launch dates in 2018 exist in the literature, this year is chosen for an exhaustive analysis on the family of feasible tours. The basic seven-planet cycler (E-M-E-M-E-M-E) is calculated and used as a basis for comparison with more complex cyclers and tours that include Venusian encounters. Table 1 shows the best combination when optimized for $\Delta v$ including Earth departure $v_\infty$. The 3.62 km/s maneuver at the second encounter with Mars is the result of a trade off between minimizing the Earth departure velocity and total trip $\Delta v$. For comparison, if Earth departure is removed from the cost and a new minima is calculated, the total trip $\Delta v$ reduces to 1.25 km/s for the gravity assist maneuvers alone at the expense of a much larger hyperbolic excess velocity at departure.

For the lowest cost trajectories studied, the largest expense is usually a series of plane change maneuvers to compensate for inclination differences between the planets. When viewing the trajectory from a direction perpendicular to the ecliptic (Figure 5 left), trajectory changes are barely noticeable and well within the possible turn angle in each planetary encounter. Viewing the trajectory isometrically with thrust vectors for the low-thrust optimization (Figure 5 right) indeed shows that most of the thrust and gravity maneuvers are perpendicular to the ecliptic. This sensitivity implies that fortuitous alignments of inclination are nearly as important as each planet's true anomaly and reinforces the hypothesis that the addition of Venus may offer opportunities to enact or avoid a plane change and thus reduce the $\Delta v$ cost of a tour.

When trajectories for an intermediate eighth or ninth planet with the same number of Earth-Mars and Mars-Earth transfers are calculated, the cost falls considerably. The lowest $\Delta v$ cost trajectory found in 2018 is a nine-planet (E-M-E-E-M-E-V-M-E) tour (Figure 6, Table 2) that requires 6.172 km/s including Earth departure for the impulse version of the trajectory and 7.262 km/s for the low-thrust counterpart. The $\sim 17\%$ increase in $\Delta v$ cost is typical for low-thrust impulse pairs in both the even-sampling and multi-objective

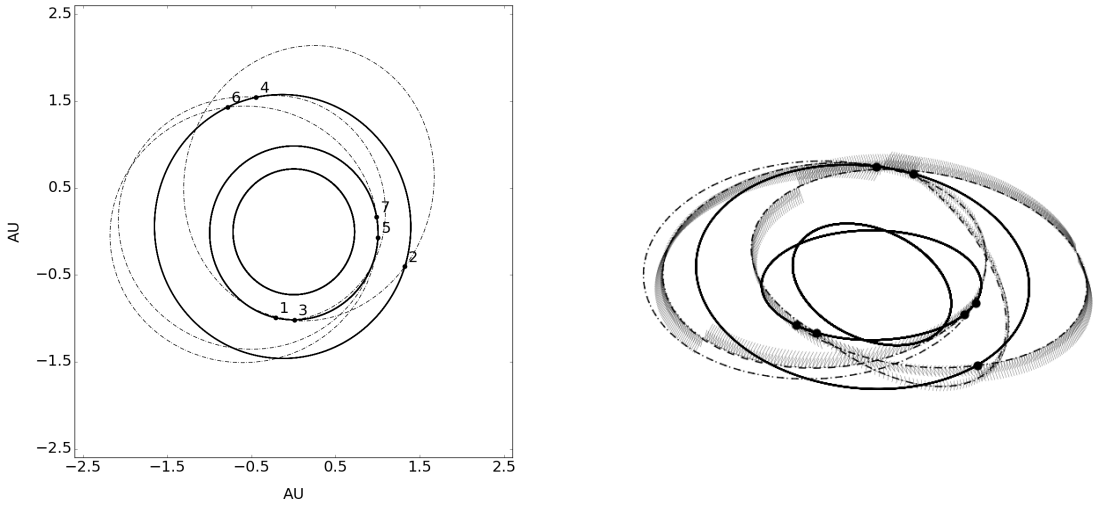


**Figure 5. Two dimensional view of the seven-planet baseline cycler trajectory described in Table 1 as viewed from the positive z direction in ecliptic coordinates (left) and in three dimensions with low thrust vectors (right) with an exaggerated scale to emphasize inclination. The orbits of Venus, Earth, and Mars are represented by thick solid ellipses. The impulse trajectory is represented by dashed lines and the low thrust trajectory is shown as a dotted line. The origin for each plot is the location of the sun.**

studies which is analytically demonstrable with the Cauchy-Schwartz inequality.[20] For tours with low cost, this difference is usually so small that the linearized estimate of the trajectory used in the low-thrust modeling is almost identical to the final solution after convergence. The slight difference in the low thrust trajectory (dashed line) and the impulse trajectory (dotted line) is again only visually significant in the z direction of ecliptic due to the necessity of a plane change maneuver. The minimum cost nine-planet solution therefore endures relatively small thrusted plane changes as shown in the isometric view (right). Compared to the base seven-planet tour, this nine-planet tour achieves a much lower earth departure $v_\infty$ as a trade against a larger maneuver at the first Mars encounter which highlights how the solution space might expand when algorithms are allowed to attempt to minimize Earth departure. Also unlike a traditional cycler trajectory, the first E-M-E cycle has an apoapsis nearly coincident with the encounter at Mars and a periapsis slightly inside the orbit of Venus which acts to reduce the TOF between the two planets. The second consecutive Earth encounter acts to shift the trajectory back to a more traditional cycler before a Venusian encounter is used to enact a ballistic plane change for the final Mars-Earth leg. One disadvantage of this solution is that the hyperbolic excess velocity grows with each encounter from 3.38 km/s at departure to as much as 18.73 km/s at final Earth arrival whereas a traditional cycle maintains consistent excess velocities due to the nearly exact repetition of parameters after a set of synodic periods.

Table 3 shows the application of the both the even-sampling and the optimization loop approach to the specified trajectories and the minimum $\Delta v$ cost in 2018. Even sampling generated results with inappropriately high $\Delta v$ for all combinations of encounters at the limit of the computational resources available. The optimization loop offered improvements that averaged over 50% with the smaller improvements mostly due to coincidental alignments.

To cull results, tours with a $\Delta v$ greater than 15 km/s using the optimization loop approach are excluded from analysis. Though not all combinations of planets that allow for the required three Earth-Mars and Mars-Earth transfers are represented, several dozen met this criteria. Additionally, alternate launch dates with similar $\Delta v$ costs are available for most tours.

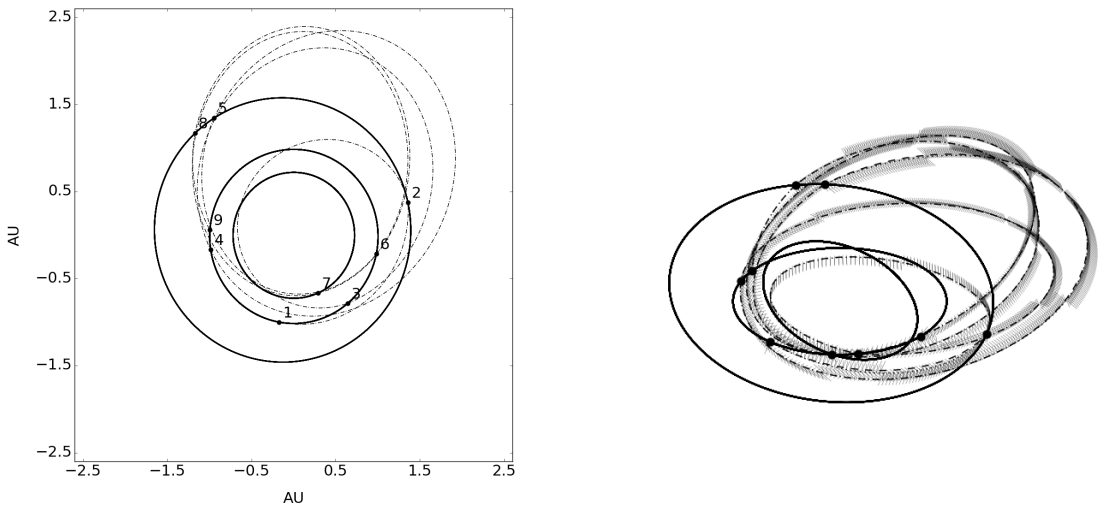


**Figure 6. The nine-planet tour described in Table 2 plotted in the same manner as Figure 5.**

| Encounter | Planet | Encounter Date | $\Delta v_{\mathrm{req,impulse}}$ | $\Delta v_{\mathrm{req,low-thrust}}$ |
|---|---|---|---|---|
| 1 | Earth | June 22, 2018 | 3.38 km/s | 3.38 km/s |
| 2 | Mars | November 14, 2018 | 2.07 km/s | 2.95 km/s |
| 3 | Earth | August 13, 2019 | 0.16 km/s | 0.21 km/s |
| 4 | Earth | April 10, 2021 | 0.00 km/s | 0.00 km/s |
| 5 | Mars | March 18, 2023 | 0.54 km/s | 0.70 km/s |
| 6 | Earth | September 21, 2023 | 0.01 km/s | 0.02 km/s |
| 7 | Venus | June 30, 2025 | 0.00 km/s | 0.00 km/s |
| 8 | Mars | January 12, 2027 | 0.00 km/s | 0.00 km/s |
| 9 | Earth | March 28, 2027 | N/A | N/A |
| Total | | | 6.17 km/s | 7.27 km/s |

**Table 2. Lowest $\Delta v$ tour found for 2018 tabulated in the same manner as Table 1.**

| Planets | Even-Sampling [km/s] | Optimization Loop [km/s] | Difference |
|---|---|---|---|
| E-V-E-M-E-M-E-M-E | 17.425 | 7.485 | -57.0% |
| E-V-M-E-M-E-M-E-E | 26.937 | 12.395 | -54.0% |
| E-V-M-E-M-E-M-V-E | 21.721 | 12.977 | -40.3% |
| E-V-M-E-M-V-E-M-E | 23.923 | 13.624 | -43.1% |
| E-V-M-V-E-M-E-M-E | 35.165 | 9.684 | -72.5% |
| E-M-E-M-E-E-M-E-E | 20.653 | 10.247 | -50.4% |
| E-M-E-M-E-E-M-V-E | 21.739 | 10.615 | -51.2% |
| E-M-E-M-E-M-E-E-E | 34.463 | 9.593 | -72.2% |
| E-M-E-M-E-M-E-M-E | 27.972 | 13.599 | -51.4% |
| E-M-E-M-E-M-E-V-E | 26.736 | 9.785 | -63.4% |
| E-M-E-M-E-M-M-E-E | 24.751 | 14.990 | -39.4% |
| E-M-E-M-E-M-V-M-E | 25.455 | 12.658 | -50.3% |
| E-M-E-M-E-M-V-V-E | 23.869 | 10.120 | -57.6% |
| E-M-E-M-E-V-E-M-E | 23.092 | 9.000 | -61.0% |
| E-M-E-M-E-V-M-E-E | 15.574 | 12.061 | -22.6% |
| E-M-E-M-E-V-M-V-E | 15.018 | 11.016 | -26.6% |
| E-M-E-M-E-V-V-M-E | 16.529 | 8.453 | -48.9% |
| E-M-E-M-V-E-M-E-E | 21.667 | 7.651 | -64.7% |
| E-M-E-M-V-E-M-V-E | 20.166 | 8.293 | -58.9% |
| E-M-E-M-V-E-V-M-E | 27.83 | 13.196 | -52.6% |
| E-M-E-M-V-M-E-M-E | 15.152 | 9.155 | -39.61% |
| E-M-E-M-V-V-E-M-E | 23.781 | 8.124 | -65.8% |
| E-M-E-V-E-M-E-M-E | 21.851 | 9.581 | -56.2% |
| E-M-E-V-M-E-V-M-E | 24.474 | 11.184 | -54.3% |
| E-M-E-V-M-V-E-M-E | 21.737 | 11.378 | -47.7% |
| E-M-E-V-V-M-E-M-E | 20.147 | 10.196 | -49.4% |
| E-M-M-E-M-E-M-V-E | 27.716 | 12.121 | -56.3% |
| E-M-M-E-M-V-E-M-E | 23.122 | 11.555 | -50.0% |
| E-M-M-M-E-M-E-M-E | 34.127 | 12.685 | -62.8% |
| E-M-M-V-E-M-E-M-E | 31.609 | 12.031 | -61.9% |
| E-M-V-E-M-E-M-E-E | 24.425 | 7.788 | -68.1% |
| E-M-V-E-M-E-M-V-E | 18.233 | 7.613 | -58.2% |
| E-M-V-E-M-E-V-M-E | 34.335 | 7.166 | -79.1% |
| E-M-V-E-M-V-E-M-E | 15.126 | 7.462 | -50.7% |
| E-M-V-V-E-M-E-M-E | 17.563 | 7.526 | -57.2 % |

**Table 3. Lowest $\Delta v$ tour found for 2018 for both the even sampling and optimization loop approach The optimization loop method resulted in lower $\Delta v$ requirements for all tours examined.**

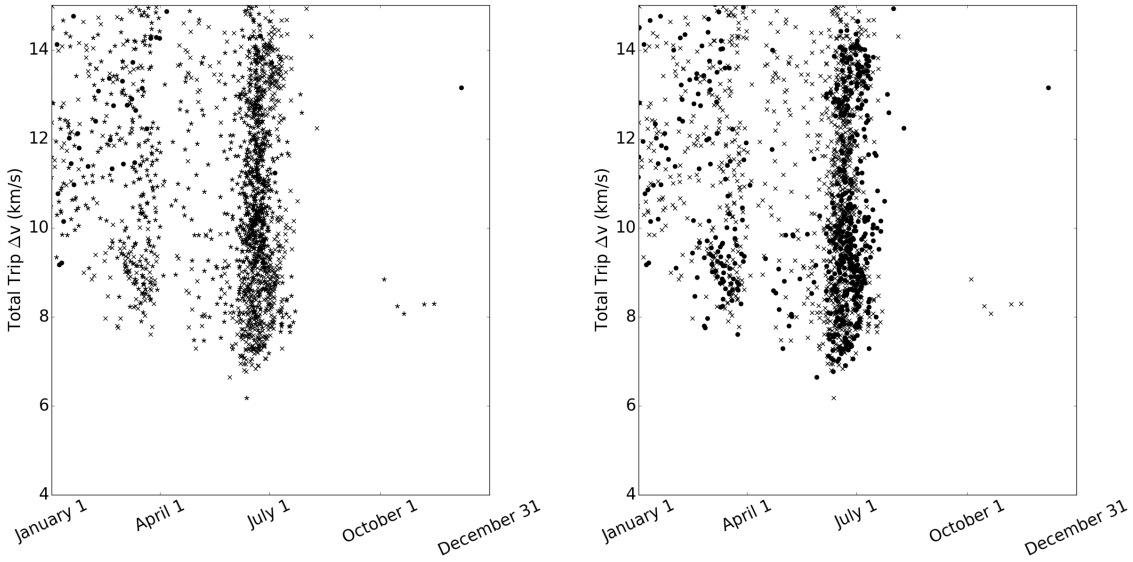


**Figure 7. Plot of $\Delta v$ versus launch date for the multi-objective optimization loop approach. Circle, cross and star markers are used for zero, one or two planets inserted into the one-synodic period cycler respectively (left). For the plot on the right, cross markers are used if the tour includes an encounter with Venus and a circle if not.**

### Multi-objective Results

Analysis of the full multi-objective function is restricted to the optimization loop approach. By varying $w_0$ and $w_1$ in Equation 6 to explore the full range of possible solutions and applying the $\Delta v$ cut off of 15 km/s, several hundred launch date solutions are generated that are not strictly coincident with an optimization of solely the $\Delta v$ cost. When plotted (Figure 7), a significant grouping of solutions from late May to late July 2018 is observed including the minima described in Table 2. Due to the flexibility of the algorithm, the initial even spacing of launch dates simulated tends to group towards the nearest low-cost alignment and vacates most of the latter half of the year.

Markers in the left panel of Figure 7 are distinguished by the number of planets inserted into the one-synodic period cycler. The best solutions throughout the year required at least one intermediate planet with the exception of two one-synodic period cycler solutions in the beginning of January. Several solutions better than the base case are observed around its June 20 launch date. When distinguished by the presence of a Venusian encounter (right), the lowest $\Delta v$ tour alternates between Venus-inclusive or Venus non-inclusive throughout the year with the notable exception of a few Venus-inclusive tours well outside the traditional 2018 Mars-Earth window. With respect to $\Delta v$, this demonstrates an opportunity to add launch dates during fortuitous alignments of Venus.

A comprehensive depiction of all three objectives is presented in Figure 8. When plotting $\Delta v$ versus the average E-M and M-E times of flight (Figure 9 left), the majority of solutions bifurcate into a group around 340 days, which are consistent with the base case solution as well as most of the tours with similar launch dates and a group around 450 days, which are consistent with the longer period cycles with periapsis near the orbit of Venus like the second half of the nine-planet tour in Table 2.

As discussed, the hyperbolic excess velocity is not independently optimized as even small values of $w_3$ resulted in unacceptably high values of $\Delta v$. However, a broad range different average $v_\infty$ at Earth and Mars appear in the existing solution space (Figure 9 right). An inverse relationship is observed between average $v_\infty$ and the best $\Delta v$ and the bulk of the tours studied have an average $v_\infty$ above 9 km/s.

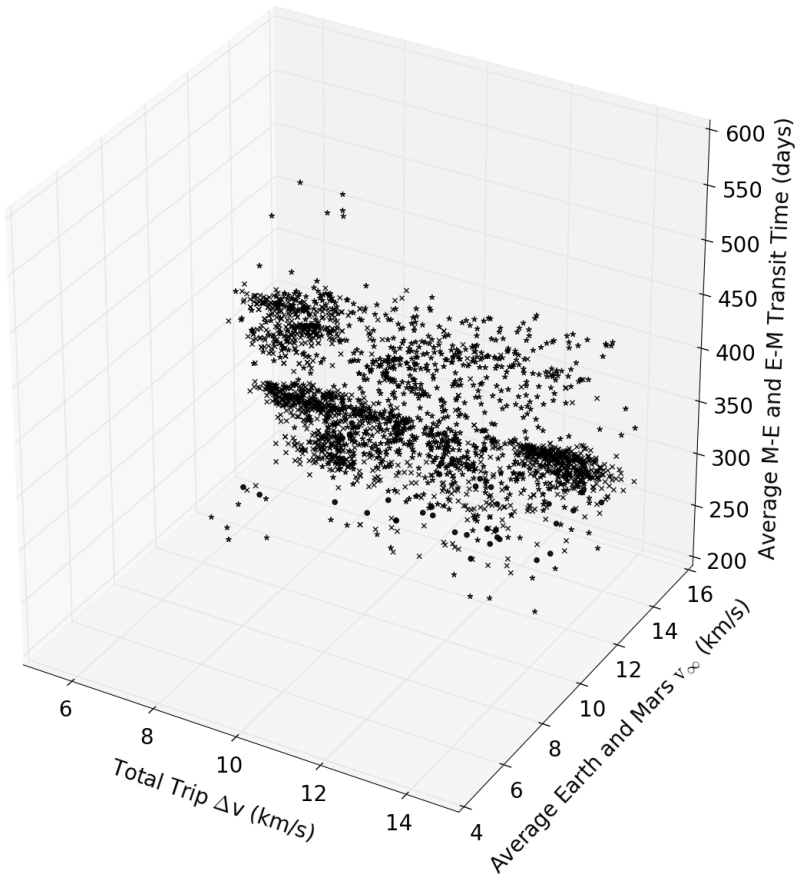


**Figure 8. Plot of $\Delta v$ versus average Earth-Mars and Mars-Earth time of flight versus average hyperbolic excess velocity and Mars and Earth. Marker usage is the same as Figure 7 left.**

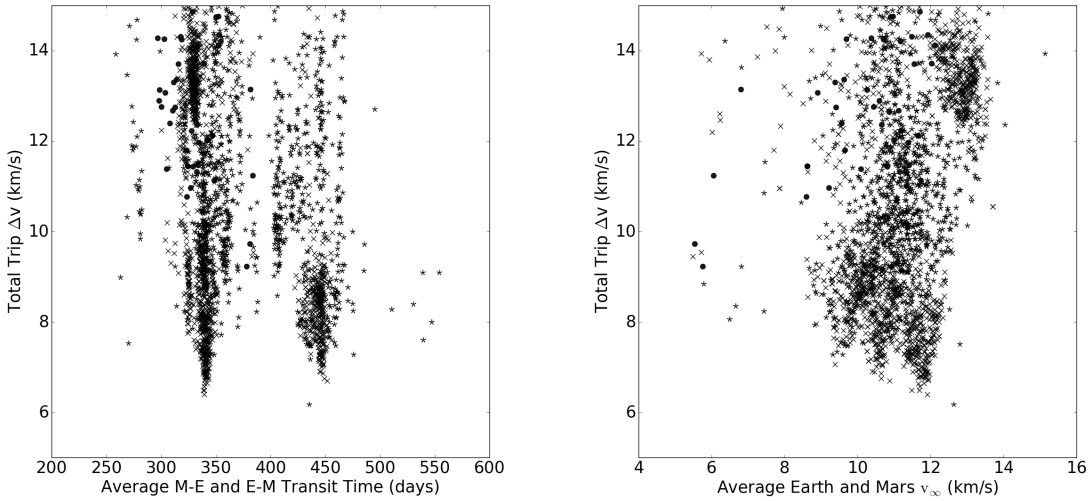


**Figure 9. Plot of $\Delta v$ versus average Earth-Mars and Mars-Earth time of flight (left) and average hyperbolic excess velocity at Mars and Earth (right). Markers are the same as Figure 7 left.**

In contrast to the seminal work of Russell and Ocampo, which gradually changes the eccentricity and inclination of established cyclers, his work allows a more flexible exploration of the parameter space at the expense of additional computational complexity. In exchange for the increased computational complexity, adding Venus to the analysis is found to contribute opportunities to reduce all three objectives of the cost function as well as provide a larger range of feasible launch dates. Solution types of this nature should therefore be included in considerations of practical applications for continuous transportation between Earth and Mars. Furthermore, whether or not Venusian encounters are included, the recursive optimization approach more readily allows trades to be made between $v_\infty$, $\Delta v$, and time of flight than an analysis confined to cycler templates.

## CONCLUSION

A new loop optimization approach to n-body planetary tours in the solar system is studied against solutions methods for the classic Mars-Earth cycler. From the initial set of three planets, the cost of a tour is optimized incrementally allowing solutions to migrate towards and between local minimum costs. The benefit of this approach is that it scales well to many planets, but it does not guarantee that the solutions found are absolute cost minima. Sampling the entire space of possible launch and encounter dates is computationally infeasible and offers poorly optimized costs. Restricting solutions for repeated Earth-Mars transfers to cyclers constrains the selection of launch dates and the TOF cost of the tour, but may result in well-optimized $\Delta v$ for an individual solution. Allowing encounters with Venus offers the opportunity to enact or avoid a plane change and may reduce the cost of an otherwise infeasible tour.

Furthermore, the flexibility of piecewise optimization within an open parameter space allows solutions to adaptively migrate between classes or cyclers or non-cycler arrangements whenever a fortuitous alignment exists. Solutions that behave in this manner such as the tour described in Figure 6 and Table 2 offer a new line of inquiry into solutions classes for Earth-Mars transport. Importantly, the method of recursive optimization easily extends to any n-body multi-planetary trajectory and can be used to ease the computational load of studies with respect to a brute-force multiple shooting method approach.

## REFERENCES


[1] Rall, C. S., "Free-Fall Periodic Orbits Connecting Earth and Mars," *Sc. D Thesis, Department of Aeronautics and Astronautics, M.I.T., October 1969*

[2] Rall, C. S., and Hollister, W. M., "Free-Fall Periodic Orbits Connecting Earth and Mars," *AIAA 9th Aeroscpace Sciences Meeting*, AIAA Paper 72-92, January 1971

[3] Aldrin, E. E, "Cyclic Trajectory Concepts," SAIC presentation to the Interplanetary Rapid Transit Study Meeting, Jet propulsion Laboratory, October 28, 1985

[4] Byrnes, D. V, Longuski J. M, and Aldrin B., "Cycler Orbit Between Earth and Mars," *Journal of Spacecraft and Rockets*, Vol. 30. No. 3, May-June 1993, pp. 334-336

[5] Friedlander, A. L., Nieho, J. C., Byrnes, D. V., and Longuski, J. M., "Circulating Transportation Orbits Between Earth and Mars," AIAA/AAS Astrodynamics Conference, Williamsburg, Virginia, August 1986, AIAA 86-2009-CP

[6] Byrnes, D. V., McConaghy, T. T., and Longuski, J. M., "Analysis of Various Two Synodic Period Earth-Mars Cycler Trajectories," AIAA/AAS Astrodynamics Specialist Conference, Monterey, CA, August 5-8 2002, AIAA 2002-4423.

[7] McConaghy T. T., Longuski, J. M. L. "Analysis of a Broad Class Mars-Earth Cycler Trajectories," *Journal of Spacecraft and Rockets*, Vol. 41, No. 4, July-August 2004

[8] Sims, J. A., and Flanagan, S. N., "Preliminary Design of Low-Thrust Interplanetary Missions," *American Astronomical Society*, Paper 99-338, August 1999

[9] McConaghy, T. T., Debban, T. J., Petropoulos, A. E., and Longuski, J. M., "Design and Optimization of Low-Thrust Trajectories with Gravity Assists," *Journal of Spacecraft and Rockets*, Vol. 40, No. 3, 2003

[10] Chen, J. K., McConaghy, T. T., Okutsu, M., and Longuski, J. M., "A Low-Thrust Version of the Aldrin Cycler," AIAA Paper 2002-4421, August 2002

[11] Chen, K. J., Landau, D. F., McConaghy, T. T., Okutsu, M., Longuski, J. M., and Aldrin, B., "Preliminary Analysis and Design of Powered Earth- Mars Cycling Trajectories," AIAA Paper 2002-4422, Aug. 2002

[12] McConaghy, T. T, Landau, D. F., Yam, C. H. Longuski "Notable Two-Synodic-Period Earth-Mars Cycler," *Journal of Spacecraft and Rockets*, Vol. 43, No. 2, March-April 2006

[13] Chen, J. K., McConaghy T. T., Landau, D. F., Longuski, J. M. "Powered Earth-Mars Cycler with Three-Synodic-Period Repeat Time," *Journal of Spacecraft and Rockets*, Vol. 42, No. 5 (2005), pp. 921–927

[14] Russell, R. P., Ocampo, C. A. "A Systematic Method for Constructing Earth-Mars Cyclers Using Direct Return Trajectories," *Journal of Guidance, Control, and Dynamics*, Vol. 27, No. 3, 2004 Vol. 42, No. 5, September-October 2005

[15] Gill, P. E., Murray, W., and Saunders, M. A., "SNOPT: An SQP Algorithm for Large Scale Constrained Optimization, SIAM Journal of Optimization, Vol. 12, No. 4, 2002, pp. 979-1006.

[16] Russell, R. P., and Ocampo "Optimization of a Broad Class of Emphemeris Model Earth-Mars Cyclers," *Journal of Guidance, Control, and Dynamics*, Vol. 29, No. 2, March-April 2006

[17] Wolfe, P., "Convergence Conditions for Ascent Methods," SIAM Review , Vol. 11, No. 2, 1969

[18] Bate, R. R, Mueller, D. D, and White, J. E., "Fundamentals of Astrodynamics," Dover Publications, Copyright 1971

[19] William Alexander J. "Sol Planetary System Data" `http://www.princeton.edu/~willman/planetary_systems/Sol`, 2012

[20] Gustafson, Eric D and Scheeres, Daniel J "Optimal timing of control-law updates for unstable systems with continuous control," *Journal of Guidance, Control, and Dynamics*, Volume 33, No. 3, pp. 878–887, 2009